Photoredox Chemistry of Keggin Dodecatungstoborate $[BW_{12}O_{40}]^{5-}$ and Role of Heterogeneous Catalysis in Hydrogen Formation†

Toshihiro Yamase* and Reiko Watanabe
Research Laboratory of Resources Utilization, Tokyo Institute of Technology, 4259 Nagatsuta, Midori-ku, Yokohama 227, Japan

Photoexcitation of the oxygen-to-tungsten charge-transfer band of $[BW_{12}O_{40}]^{5-}$ in the presence of CH_3OH leads to the formation of $[BW_{12}O_{40}]^{6-}$, H_2, and formaldehyde at $2.0 < pH < 9.4$, with a resultant liberation of protons from CH_3OH. Low values (1.6—1.8) of the kinetic isotope effect imply that the electron transfer from CH_3OH to photoexcited $[BW_{12}O_{40}]^{5-}$ occurs before proton loss, rather than that the cleavage of the alcohol C–H bond is rate determining. A value (0.43 eV) of the electron-transfer integral between adjacent tungsten sites for the unpaired electron in $[BW_{12}O_{40}]^{6-}$ was estimated from the temperature dependence of the e.s.r. linewidth. The formation of H_2 can be explained in terms of two-electron reduction species, $[BW_{12}O_{40}]^{7-}$, formed by either photodisproportionation of $[BW_{12}O_{40}]^{6-}$ or photoredox reaction of $[BW_{12}O_{40}]^{6-}$ with CH_3OH. In highly acidic solutions ($pH \leqslant 2$), protonation of $[BW_{12}O_{40}]^{6-}$ is dominant and is followed by successive disproportionations to the six-electron reduction species which exhibits an oxidation potential more positive than the reduction potential of water. This results in a decrease in the rate of formation of H_2 and is associated with protonation of $[BW_{12}O_{40}]^{7-}$. Heterogeneous catalysts such as Pt and RuO_2 scavenge $[H_2BW_{12}O_{40}]^{5-}$, the precursor of the six-electron reduction species, leading to an increase in the rate of formation of H_2.

In the course of our studies on the photochemistry of polyoxometalates, which constitute an interesting family of potential photosensitizers and relay species in redox cycles for the chemical conversion of light energy, photoredox reactions of isopolymetalates with water, carboxylic acids, alcohols, alkynes, and alkenes have been described.[1–5] As an extension of these studies to the heteropolyoxometalates, we report here the photoredox properties of dodecatungstoborate, $[BW_{12}O_{40}]^{5-}$, with methanol. Photochemical production of hydrogen by Keggin heteropolyoxotungstates such as $[PW_{12}O_{40}]^{3-}$, $[SiW_{12}O_{40}]^{4-}$, and $[H_2W_{12}O_{40}]^{6-}$ has been reported:[6–9] it was thermodynamically favourable only at high proton concentrations, and heterogeneous Pt seemed to enhance the rate. On the other hand, we have found that $[BW_{12}O_{40}]^{5-}$ is capable of forming H_2 from alcohols photochemically with (at $pH \leqslant 2.0$) and without (at $2.0 < pH < 9.4$) heterogeneous catalysts such as Pt, RuO_2, and IrO_2.[10] The details now presented allow several generalizations regarding the photoredox properties of Keggin heteropolyoxotungstates in aqueous solutions, and a better understanding of the photochemistry of heteropolyanions.

Experimental

Pentapotassium dodecatungstoborate pentadecahydrate $K_5[BW_{12}O_{40}]\cdot 15H_2O$ was prepared according to ref. 11 and recrystallized three times from warm water at 60 °C. Thermogravimetric analysis (Rigaku, thermoflex TG-DGC) was used for the determination of water of crystallization (Found: B, 0.30; K, 5.50; W, 66.4; H_2O, 8.15. Calc. for $BK_5O_{40}W_{12}\cdot 15H_2O$: B, 0.35; K, 5.90; W, 66.4; H_2O, 8.15%). The ^{183}W and ^{17}O n.m.r. spectra (on JEOL FX 450 and FX 100 spectrometers) confirmed the α-Keggin structure of $[BW_{12}O_{40}]^{5-}$:[12] $\delta(^{183}W)$ −130.08 (s) relative to $Na_2[WO_4]$ at pD 0.3; $\delta(^{17}O)$ 737.0 and 408.1 p.p.m. relative to water at pD 5.4, signal intensity *ca.* 1:2.

Colloidal Pt was prepared by reduction of H_2PtCl_6 with sodium citrate, followed by stirring with Amberlite-MB-3 exchange resin to remove the citrate.[13] [$^2H_4$]Methanol (CD_3OD, >99.5%D, Aldrich Chem. Co.) and deuteriated water (D_2O, >99.9%D, Merck Co.) were used without further purification. All other reagents were at least analytical grade and were used as supplied.

A 500-W super-high-pressure mercury lamp in conjunction with filters was used as a light source. Light intensities at 313 nm were measured using potassium ferrioxalate actinometry.[14] Sample solutions (5 cm^3) for long-term photolyses in Pyrex tubes were deaerated with solvent-saturated nitrogen or argon. Analysis for W^V in the photolyte was carried out at room temperature by iodometry under an atmosphere of nitrogen, and resulted in the disappearance of the colour due to W^V. Gas chromatography (Hitachi 164) on a Carbosieve S column was employed for analysis of hydrogen. Formaldehyde in photolytes was determined by means of the acetylacetone procedure.[15] All procedures for colourimetric analysis were carried out after decolouration of the W^V by admission of oxygen, and blanks were prepared with solutions kept in the dark. The evacuation to 10^{-4} Torr of solutions for measurements of absorption and e.s.r. spectra and flash photolysis was carried out by several freeze–pump–thaw cycles. Solutions for electrochemical measurements were flushed with nitrogen to exclude oxygen.

Electronic spectra were recorded on a Hitachi 624 or 200-10 spectrometer. *X*-Band e.s.r. spectra were recorded on a Varian E12 spectrometer equipped with an Oxford Instruments cryostat (ESR 900) in order to perform experiments down to 20 K. Polarograms were recorded on EG and G PAR (174 A and 303) instruments and a standard cell with an Ag–AgCl reference electrode. Cyclic voltammograms were measured with a potentiostat/galvanostat (Hokuto Denko HA-301) and a function generator (Nikko Keisoku NFG-3), and all measure-

† *Non-S.I. units employed:* Torr ≈ 133 Pa, eV ≈ 1.6×10^{-19} J; G = 10^{-4} T.

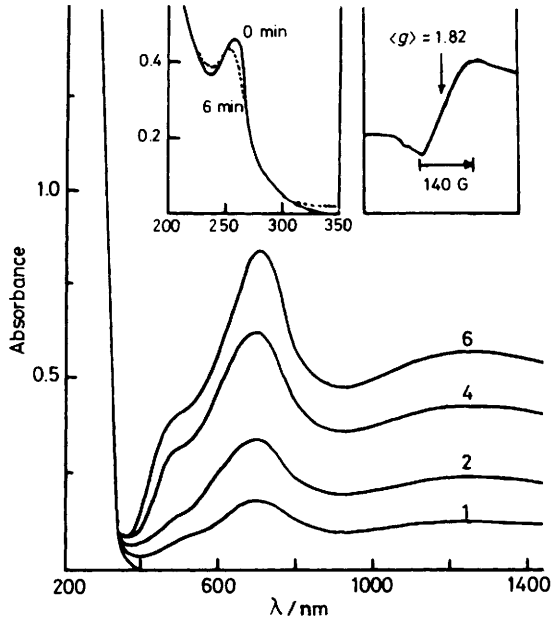

Figure 1. Spectral changes upon 313-nm light irradiation of a deaerated solution (pH 5.4) containing 1.0 mmol dm^{-3} $K_5[BW_{12}O_{40}]$ and 2.5 mol dm^{-3} CH_3OH. Times (min) are indicated on the curves. Optical pathlength: 10 mm. Inserts: spectral changes at 200—350 nm (optical pathlength 0.1 mm) and e.s.r. spectrum of the photolyte (irradiation time 10 min) at 77 K

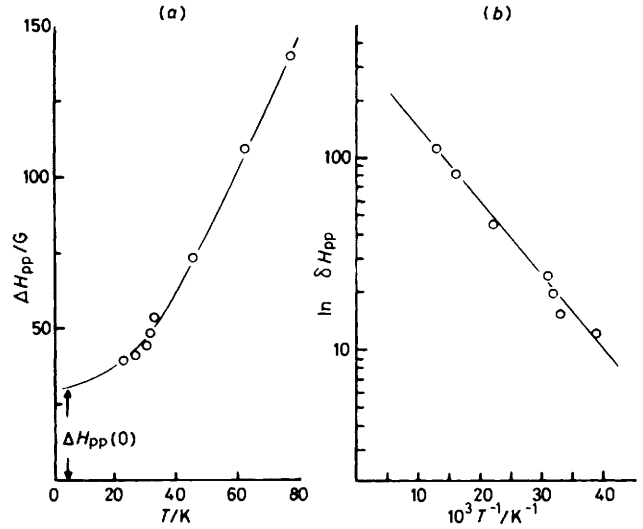

Figure 2. Temperature dependence (*a*) of the e.s.r. linewidth of $[BW_{12}O_{40}]^{6-}$ and (*b*) of ln δH_{pp} where $\delta H_{pp} = \Delta H_{pp} - \Delta H_{pp}(0)$ corresponds to the temperature-dependent part of ΔH_{pp}

ments were made using an amalgamated gold working electrode, a platinum-wire counter electrode, and a saturated calomel reference electrode (s.c.e.). For controlled-potential reduction experiments, mercury, platinum plate, and silver wire or Ag–AgCl (saturated KCl) were used as working, counter, and reference electrodes, respectively. All electric potentials quoted are with reference to Ag–AgCl (saturated KCl). Conductivity measurements were done at 291 ± 1 K with a Delica a.c. model 12K Impedance Bridge (frequency: 10^3 Hz). The flash-photolysis experiment was carried out with a Xenon Corp. model 720 flash-photolysis apparatus. Two EP-5-100 C lamps were fired at 320 J per pulse. The lifetime for the flash pulse was 100 μs. A transmitting glass filter (Toshiba VY-43, cut-off, λ < 430 nm) was inserted between the monitoring lamp and the reaction cell (optical pathlength 100 mm).

Results and Discussion

Characterization of $[BW_{12}O_{40}]^{6-}$. A solution of $[BW_{12}O_{40}]^{5-}$ in aqueous methanol (pH 5.4) showed an intense absorption band at 255 nm ($\varepsilon = 4.50 \times 10^4$ dm^3 mol^{-1} cm^{-1}), due to the oxygen-to-tungsten charge transfer (ligand-to-metal charge transfer, l.m.c.t.) involving the terminal W^{VI}=O bond.[16] On exposure of the deaerated solutions to light of a wavelength (313 nm) corresponding to the edge of the 255-nm l.m.c.t. band, $[BW_{12}O_{40}]^{6-}$ was produced, showing $\lambda_{sh} = 500$ nm ($\varepsilon = 1.00 \times 10^3$ dm^3 mol^{-1} cm^{-1}) and $\lambda_{max.} = 695$ (2.00×10^3) and 1 250 nm (1.38×10^3 dm^3 mol^{-1} cm^{-1}) due to the *d–d*, *d–d* or intervalence, and intervalence transitions respectively.[16] It also gave a characterstic e.s.r. signal as a broad singlet ($g = 1.82$) without hyperfine splitting (h.f.s.) at 77 K. The absence of CH_3OH resulted in no steady-state photoreduction of $[BW_{12}O_{40}]^{5-}$. Figure 1 shows typical absorption spectra and the e.s.r. spectrum of the photolyte. Upon the photoreduction the 255-nm l.m.c.t. band was only reduced in intensity. This is in contrast with the case of the decatungstate $[W_{10}O_{32}]^{4-}$, for which the characteristic l.m.c.t. band at 323 nm in CH_3CN disappeared completely.[1] The e.s.r. signal intensity increased with the steady-state photolysis and reached a limiting value. Similar behaviour during the photolysis was observed for the absorbance at 695 nm. The e.s.r. linewidth decreased with decreasing temperature in the range 20—100 K where each e.s.r. spectrum seemed to be isotropic, although that of $[BW_{12}O_{40}]^{6-}$ was orthorhombic at 14 K.[17] A plot of the peak-to-peak half-width, ΔH_{pp}, *vs.* temperature, T, is presented in Figure 2. The broadening of the e.s.r. spectrum with temperature indicates that thermal electron delocalization occurs when the paramagnetic tungsten(v) ion is surrounded by other tungsten(vi) ions.[18] The 'hopping' of the unpaired electron between the W^V and W^{VI} can be activated either optically, leading to the intervalence c.t. band around 1 250 nm, or thermally, leading to a broadening of the e.s.r. signal above 20 K.[19] The optical activation energy, $E_{opt} = 0.992$ eV, was deduced from the position of the intervalence charge-transfer band. The thermal activation energy, E_{th}, and the electron-transfer integral, J, could be deduced from an analysis of the dependence of ΔH_{pp} on T (Figure 2):[18] ΔH_{pp} can be expressed as the sum of two

$$\Delta H_{pp}(T) = \Delta H_{pp}(0) + \delta H_{pp}(T) \qquad (1)$$

terms [equation (1)].[20] The temperature-independent linewidth, $\Delta H_{pp}(0)$, is mainly due to dipolar interactions between paramagnetic ions together with non-resolved hyperfine couplings and ligand-field heterogeneities leading to a g-value distribution. It corresponds to the linewidth at 0 K and can be obtained by extrapolation of a plot of $\Delta H_{pp}(T)$ against T [Figure 2(*a*)]. The term $\delta H_{pp}(T)$ is proportional to the hopping frequency of the unpaired electron, ν_h, which can be expressed

$$\nu_h = \nu_0 \exp(-2\alpha R) \cdot \exp(-E_{th}/kT) \qquad (2)$$

as in equation (2) where α is the rate of the wavefunction decay, R the distance between two tungsten ions, and E_{th} the thermal activation energy for hopping.[21] The first exponential corresponds to the tunnelling effect and the second one to the thermally activated hopping. Thus $E_{th} = 0.004$ eV can be obtained from a plot [Figure 2(*b*)] of $\delta H_{pp}(T)$ *vs.* $1/T$ in the high-temperature region where the spin–spin relaxation time, t_2, is much longer than the spin–lattice relaxation time, t_1.[22] Then, the transfer integral $J = 0.43$ eV between two tungsten sites can

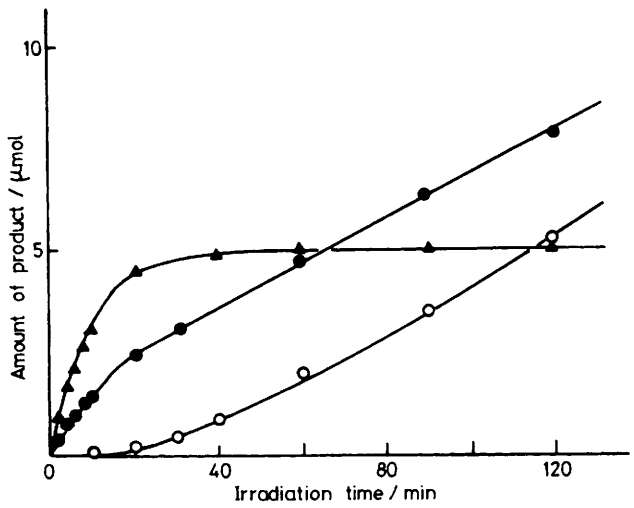

Figure 3. Plots of the amounts of products against irradiation time (313-nm light) for a deaerated solution (5 cm^3) containing 1.0 mmol dm^{-3} $K_5[BW_{12}O_{40}]$ and 2.5 mol dm^{-3} CH_3OH: HCHO (●); W^V (▲); and H_2 (○). Incident light intensity: 8.2 μE min^{-1}

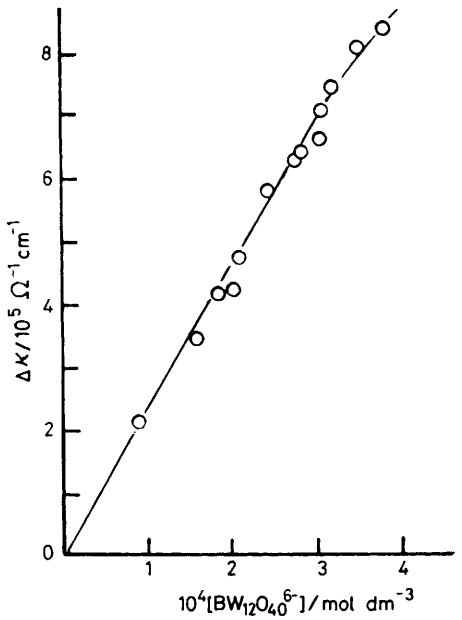

Figure 4. Correspondence between $[BW_{12}O_{40}]^{6-}$ formation and the increase (Δκ) in electrical conductivity

Table. Quantum yields (φ)[a] of HCHO for deaerated solutions (pH 5.4) containing 1.0 mmol dm^{-3} $K_5[BW_{12}O_{40}]$ and various concentrations of CH_3OH or CD_3OD

$[CH_3OH]$/ mol dm^{-3}	φ_H	$[CD_3OD]$[b]/ mol dm^{-3}	φ_D	φ_H/φ_D
0.62	4.1×10^{-3}			
0.84	5.9×10^{-3}	0.84	3.5×10^{-3}	1.7
1.24	9.2×10^{-3}	1.24	5.0×10^{-3}	1.8
2.47	1.4×10^{-2}	2.47	8.6×10^{-3}	1.6
4.94	2.2×10^{-2}			

[a] φ Measured for irradiation with 313-nm light for 20 min (8.2 μE min^{-1}). [b] The CD_3OD must be changed to CD_3OH due to H–D exchange in aqueous solution.

be calculated from expression (3).[23] The high value of J is due to the large extension of the tungsten 5*d* orbitals.

$$J = \tfrac{1}{2}E_{opt} - (E_{opt}E_{th})^{\frac{1}{2}} \quad (3)$$

Other Photoproducts.—Formaldehyde was formed as a two-electron oxidation product. Hydrogen, as a two-electron reduction product, was evolved after about 100% reduction to W^V. This suggests that its formation can be induced by the photolysis of $[BW_{12}O_{40}]^{6-}$ in conjunction with the fact that the 255-nm l.m.c.t. band was hardly affected on formation of $[BW_{12}O_{40}]^{6-}$ (Figure 1). A stoicheiometric relationship between the yields of HCHO, H_2, and W^V was maintained during the photolyses as shown in Figure 3. No ethylene glycol, CO_2, or CO was detected. The quantum yields (φ) of HCHO and W^V at the initial stage of the photolysis of the sample solution (pH 5.4) containing 1.0 mmol dm^{-3} $K_5[BW_{12}O_{40}]$ and 2.5 mol dm^{-3} CH_3OH were 0.014 and 0.027, respectively. The yield was almost unchanged upon variations of the 313-nm light intensity and the initial concentration of $[BW_{12}O_{40}]^{5-}$. The photolysis led to an increase in the electrical conductivity due to the liberation of protons from CH_3OH. After the photolysis the conductivity of the photolyte remained constant. The conductivity increase, Δκ, was approximately in proportion to the concentration of $[BW_{12}O_{40}]^{6-}$ produced, as shown in Figure 4. The concentration ratio of the liberated H^+ and W^V in the photolyte was *ca.* 7:10 when the limiting equivalent ionic conductance for H^+ at 298 K, 350 Ω^{-1} cm^2 $equiv.^{-1}$ was taken.[24] Admission of oxygen to the photolyte decreased the conductivity which approached its magnitude before the photolysis, accompanied by the disappearance of the blue colour.

The effect of the methanol concentration on φ for HCHO is shown in the Table together with the results of deuterium-labelling studies. A linear Stern–Volmer relationship between $1/\varphi$ and $1/[CH_3OH]$ was observed and a kinetic isotope effect of $\varphi_H/\varphi_D = 1.6$—1.8 was measured. This low value of φ_H/φ_D for the photoredox reaction of $[BW_{12}O_{40}]^{5-}$ with methanol implies that the electron transfer occurs before proton loss and the cleavage of a C–H bond is not rate determining, since a kinetic isotope effect of 16 has been reported for the oxidation of benzaldehyde to benzoic acid by a metal complex under conditions where the C–H cleavage is clearly rate determining.[25]

The catalytic turnover, defined as the ratio of the amount of HCHO obtained to the initial amount of $[BW_{12}O_{40}]^{5-}$, is 12 after 36 h of photolysis in the presence of 2.5 mol dm^{-3} CH_3OH with 313-nm light at room temperature. Addition of Pt or RuO_2 to the solution ($2.0 < pH < 6.5$) gave no observable increase in the rate of formation of H_2, which is in contrast to the case for a highly acidic solution described below.

Effect of Solution pH.—A polarogram of $K_5[BW_{12}O_{40}]$ in a supporting electrolyte of 0.1 mol dm^{-3} $NaClO_4$ (pH 5.4) showed two reversible one-electron reduction waves at −0.51 and −0.75 V *vs.* Ag–AgCl. The half-wave potential ($E_{\frac{1}{2}}$) for the first wave was essentially unaltered in the range pH 2.0—9.4, and $E_{\frac{1}{2}}$ ($= -0.69 - 0.01$ pH) for the second wave changed slightly over the same pH range. Under more acidic conditions ($pH \leqslant 2$), each of the two one-electron reduction waves was replaced by a six-electron reduction wave ($E_{\frac{1}{2}} = -0.52 - 0.06$ pH and $-0.62 - 0.10$ pH). Controlled-potential coulometry at −0.59 V *vs.* Ag–AgCl at pH 0.3 indicated clearly that the number of moles of electrons transferred per mol of $[BW_{12}O_{40}]^{5-}$ was six for the reduction process. Cyclic voltammograms of $[BW_{12}O_{40}]^{5-}$ at pH 0.5 at two potential scan rates are shown in Figure 5: the peak currents were approximately proportional to the square root of the potential scan rate, as expected theoretically.[26] There are two quasi-reversible six-electron redox waves at scan rates higher than 10 V s^{-1}, whereas the cyclic voltammograms at scan rates lower than 2 V s^{-1} are

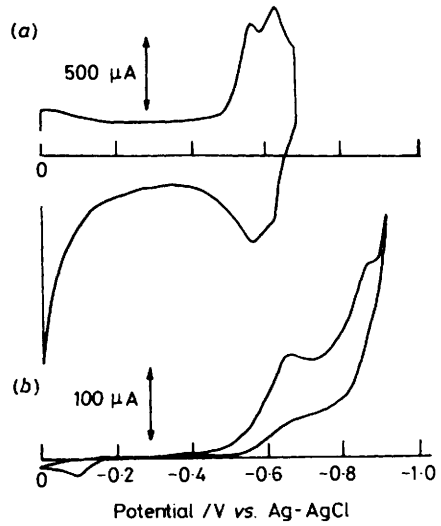

Figure 5. Cyclic voltammograms at an amalgamated gold electrode for a deaerated solution containing 1.0 mmol dm^{-3} $K_5[BW_{12}O_{40}]$, 0.1 mol dm^{-3} $NaClO_4$, and 2.5 mol dm^{-3} CH_3OH at pH 0.5. Scan rate: (*a*) 100 Vs^{-1}, (*b*) 50 mV s^{-1}

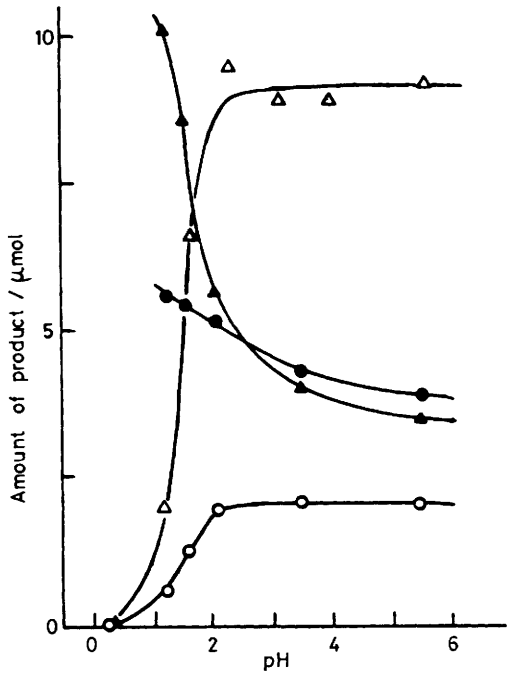

Figure 6. pH Dependence of the amounts of products after photolysis (313 nm) for 1 h of a deaerated solution (5 cm^3) containing 1.0 mmol dm^{-3} $K_5[BW_{12}O_{40}]$ and 2.5 mol dm^{-3} CH_3OH: HCHO (●), W^V (▲), H_2 (○). Δ, E.s.r. signal intensity (arbitrary units) at 77 K for the photolyte containing 0.5 mmol dm^{-3} (after photolysis of the above solution). Incident light intensity: 8.2 μE min^{-1}

irreversible, the anodic peaks being of lower magnitude and shifted toward more positive potentials around −0.1 V *vs.* Ag–AgCl. The deviation of the *i vs. E* curves from the quasi-reversible pattern at low scan rates indicates that the six-electron reduction product undergoes an irreversible postchemical reaction to give a stable species exhibiting more positive formal oxidation potentials. Polarograms of $[BW_{12}O_{40}]^{5-}$ at pH >6.5 began to diminish in height due to decomposition to mononuclear species and the waves

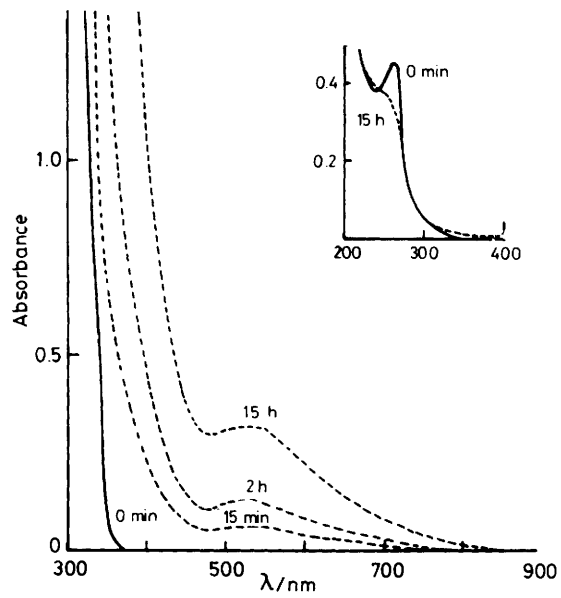

Figure 7. Spectral changes upon irradiation (313-nm light) of a deaerated solution containing 1.0 mmol dm^{-3} $K_5[BW_{12}O_{40}]$ and 2.5 mol dm^{-3} CH_3OH at pH 0.3. Times are indicated on the curves. Optical pathlength: 10 mm. Insert: spectral changes at 200—400 nm (optical pathlength 0.1 mm)

disappeared completely at pH 12.0. These electrochemical observations are in good agreement with the results obtained by Fruchart and Hervé.[27]

The yield of HCHO increased with decreasing solution pH, while the yield of H_2 decreased drastically at pH < 2 with a corresponding increase in the yield of W^V. The pH dependence of the intensity of the e.s.r. signal arising from $[BW_{12}O_{40}]^{6-}$ at constant concentration of W^V was similar to that of the hydrogen formation. Representative data are shown in Figure 6. The steady-state photoredox reaction of $[BW_{12}O_{40}]^{5-}$ with CH_3OH at pH ≤2 led to the appearance of new absorption bands around 500—550 nm as shown in Figure 7. The analysis for W^V in the photolyte after prolonged photolysis of $[BW_{12}O_{40}]^{5-}$ in the presence of 2.5 mol dm^{-3} CH_3OH at pH ≤2 indicated the addition of six electrons to $[BW_{12}O_{40}]^{5-}$. The absorption peaks around 500—550 nm were also observed upon controlled-potential electrolysis at the potential corresponding to the first six-electron reduction step at pH ≤2. Therefore, it is clear that the photoreduction product at pH ≤2 is the stable six-electron reduction species which will be e.s.r.-silent (Figure 6). The drastic decrease in the yield of H_2 at pH ≤2 can thus be attributed to the formal oxidation potential of the stable six-electron reduction species produced by the interconversion of unstable six-electron reduction species, which is more positive than the reduction potential (−0.22 −0.06 pH) of water (Figure 5).

The photolysis at pH ≤2 in the presence of Pt or RuO_2 led to an increase in the rate of hydrogen formation which was greater at higher catalyst concentrations, indicating that the heterogeneous catalysts scavenge the precursor of the stable six-electron species, the formal oxidation potential of which is more negative than the reduction potential of water. The effect of RuO_2 on the formation of H_2 at pH 0.3 is shown in Figure 8. A large amount of RuO_2 (10 mg per 5 cm^3) at pH 0.3 brought about no steady-state formation of the six-electron reduction species in the photolyte.

Photolysis of $[BW_{12}O_{40}]^{6-}$.—When a deaerated solution

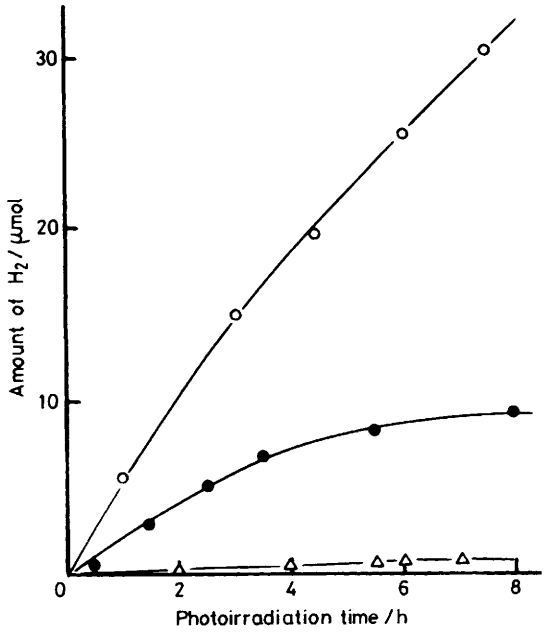

Figure 8. Effect of RuO_2 on the formation of H_2 upon photolysis (313 nm) of deaerated solution (5 cm^3) containing 1.0 mmol dm^{-3} $K_5[BW_{12}O_{40}]$ and 2.5 mol dm^{-3} CH_3OH at pH 0.3. Incident light intensity: 8.2 μE min^{-1}. Amount of RuO_2 added: 0 (△), 3.8 (●), and 10 mg (○)

containing 1.0 mmol dm^{-3} $[BW_{12}O_{40}]^{6-}$, prepared by controlled-potential reduction of 1.0 mmol dm^{-3} $K_5[BW_{12}O_{40}]$ at −0.60 V *vs.* Ag–AgCl in 0.1 mol dm^{-3} $NaClO_4$ and 1.0 mol dm^{-3} CH_3CO_2H–CH_3CO_2Na (pH 4.7), was exposed to 313-nm light, $[BW_{12}O_{40}]^{5-}$ was regenerated and was accompanied by formation of H_2 ($\varphi_{H_2} = 6.5 \times 10^{-4}$) in 1:2 molar ratio, as shown in Figure 9(*a*). The yield φ_{H_2} decreased with increasing pH at pH >7 as shown in Figure 9(*b*). The addition of 2.5 mol dm^{-3} CH_3OH to the sample solution led to an increase in φ_{H_2} (5.0×10^{-3} at pH 4.7). U.v. photolysis of $[BW_{12}O_{40}]^{6-}$ at pH >9.4 did not give H_2 but there was a change in the absorption spectrum. Figure 9(*c*) shows the spectral changes accompanying photolysis of 1.6×10^{-4} mol dm^{-3} $[BW_{12}O_{40}]^{6-}$ in the presence of 2.5 mol dm^{-3} CH_3OH at pH 11.3 and 695 nm. The ion $[BW_{12}O_{40}]^{6-}$ is very stable at pH >2 even in strongly alkaline solutions (2 mol dm^{-3} KOH).[27] Therefore, the decrease in yield of H_2 upon photolysis of $[BW_{12}O_{40}]^{6-}$ at pH >7 results from the close balance between $E_{\frac{1}{2}}$ (= −0.69 − 0.01 pH) of $[BW_{12}O_{40}]^{6-}$ and the reduction potential (−0.22 − 0.06 pH) of water. Thus, the 1:2 photoproduct molar ratio [Figure 9(*a*)] shows that $[BW_{12}O_{40}]^{6-}$ photodisproportionates to $[BW_{12}O_{40}]^{5-}$ and $[BW_{12}O_{40}]^{7-}$, followed by the rapid redox reaction between $[BW_{12}O_{40}]^{7-}$ and water to yield $[BW_{12}O_{40}]^{5-}$ and H_2 at pH ≤9. The ion $[BW_{12}O_{40}]^{7-}$ shows $\lambda_{max.} = 630$ nm and $\varepsilon = 3.38 \times 10^3$ dm^3 mol^{-1} cm^{-1} [Figure 9(*c*)]. Photoexcitation of the *d–d* or intervalence electron-transfer bands of $[BW_{12}O_{40}]^{6-}$ brought about no disproportionation of $[BW_{12}O_{40}]^{6-}$.

Reaction of $[BW_{12}O_{40}]^{5-}$ or $[BW_{12}O_{40}]^{6-}$ with CH_3CO_2H was negligible, in contrast to $[Mo_7O_{24}]^{6-}$ which exhibited a photoredox reaction with water.[3]

Photoreaction Schemes.—The acidification (to pH ≤2) of blue $[BW_{12}O_{40}]^{6-}$ solutions (pH >2) by HCl resulted in a brown colour ($\lambda_{max.}$ = 500—550 nm) due to the formation of the six-electron reduction species at room temperature. The spectral change occurred more rapidly at higher acid concentrations. Furthermore, the e.s.r. signal intensity for the photolyte at pH ≤2 decreased with the postreaction of the paramagnetic species to the brown six-election reduction species in the dark. In conjunction with the fact that the photoredox reaction between $[BW_{12}O_{40}]^{5-}$ and CH_3OH at 1.0 < pH ≤ 2.0 gave transient blue $[BW_{12}O_{40}]^{6-}$ which was subsequently converted into the brown six-electron reduction species in the dark, these results support the proposal by Fruchart and Hervé[27] that 6 mol of one-electron reduction species dismute to 1 mol of the six-electron reduction species and 5 mol of the oxidized species at pH <3. Therefore, the occurrence of the dismutation of $[BW_{12}O_{40}]^{6-}$ to the six-electron reduction species in strongly acidic media can be explained in terms of the protonation of $[BW_{12}O_{40}]^{6-}$ which will diminish the negative charge on the anions and reduce Coulombic repulsion, since there was no observable disproportionation of $[BW_{12}O_{40}]^{6-}$ in the dark at pH >2.

Unfortunately, flash photolysis of $[BW_{12}O_{40}]^{5-}$ in the presence of CH_3OH did not result in any observable transient absorption, probably due to the low quantum yield of the blue species. However, flash photolysis of a deaerated solution containing 4×10^{-5} mol dm^{-3} $H_3PW_{12}O_{40}$ and 7.4 mol dm^{-3} CH_3OH at pH 2.9 resulted in the disproportionation of photochemically produced one-electron reduction species

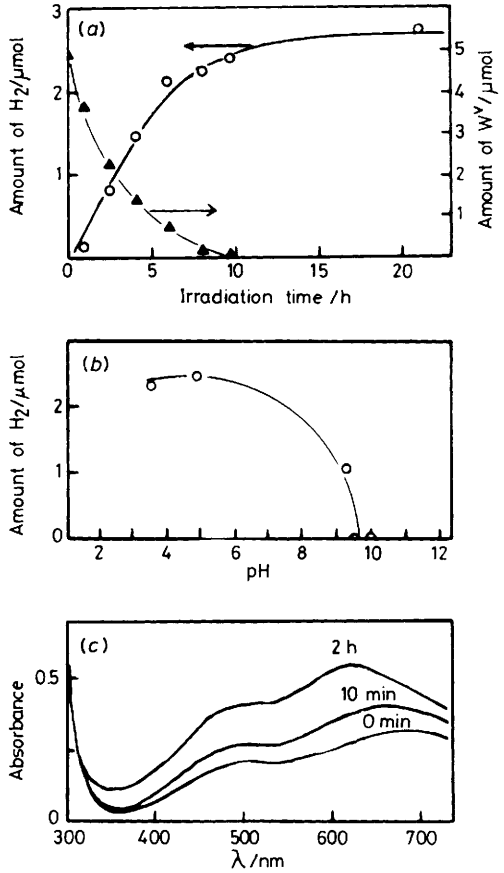

Figure 9. Photolysis (313 nm, light intensity 8.2 μE min^{-1}) of a $[BW_{12}O_{40}]^{6-}$ solution. (*a*) Plots of the amounts of products against the irradiation time for a deaerated solution (5 cm^3) containing 1.0 mmol dm^{-3} $[BW_{12}O_{40}]^{6-}$, 0.1 mol dm^{-3} $NaClO_4$, and 1.0 mol dm^{-3} CH_3CO_2H–CH_3CO_2Na at pH 4.7: H_2 (○); W^V (▲). (*b*) Amount of H_2 produced upon prolonged photolysis of solution (*a*) at various pH values. (*c*) Spectral changes for a deaerated solution containing 0.16 mmol dm^{-3} $[BW_{12}O_{40}]^{6-}$, 0.1 mol dm^{-3} $NaClO_4$, and 2.5 mol dm^{-3} CH_3OH at pH 11.3. Times are indicated on the curves. Optical pathlength: 10 mm

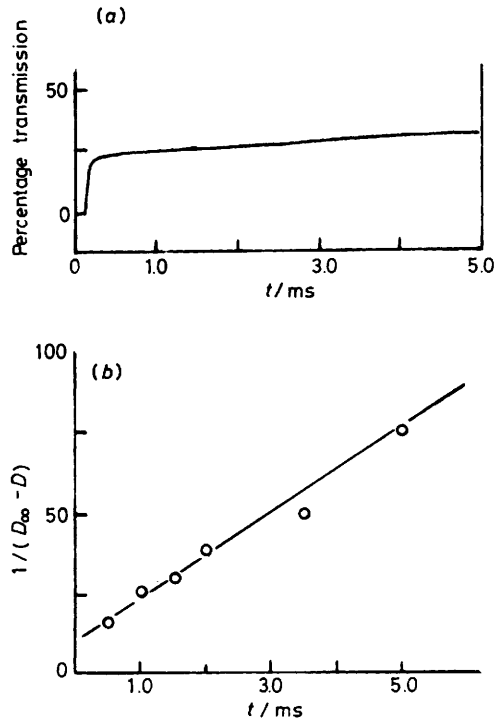

Figure 10. Flash photolysis of a deaerated solution containing 4.0×10^{-5} mol dm^{-3} $H_3PW_{12}O_{40}$ and 7.4 mol dm^{-3} CH_3OH. (*a*) Oscilloscope trace at 750 nm; (*b*) second-order kinetics

($\lambda_{max.} = 750$ nm) to two-electron reduction species, as shown in Figure 10: after the flash the absorption at 750 nm increased with time in two steps. Initially the absorbance at 750 nm due to the one-electron reduction species increased within the lifetime (100 μs) of the photoflash and further increase led to a stable blue solution. The latter absorption increase over a period of several milliseconds followed second-order kinetics and was attributed to the disproportionation (4). Using $\varepsilon_{750} =$

$$2[PW_{12}O_{40}]^{4-} \xrightarrow{k} [PW_{12}O_{40}]^{5-} + [PW_{12}O_{40}]^{3-} \quad (4)$$

2.0×10^3 dm^3 mol^{-1} cm^{-1} for $[PW_{12}O_{40}]^{4-}$ we calculated the rate constant for reaction (4) as $k = 6.4 \times 10^7$ dm^3 mol^{-1} s^{-1}. Similar behaviour has been discussed for the $[W_{10}O_{32}]^{4-}$ system.[1]

The dismutation pathway of protonated $[BW_{12}O_{40}]^{6-}$ to the stable six-electron reduction species involves transient formation of the protonated two-electron reduction species $[H_2BW_{12}O_{40}]^{5-}$, which will be capable of reducing water. Accordingly, the effectiveness of the heterogeneous catalyses on the formation of H_2 at pH $\leqslant 2$ can be associated with the stabilization of this protonated species, since $[H_2BW_{12}O_{40}]^{5-}$ is readily adsorbed on the heterogeneous metal oxide catalysts (probably PtO_2 for the surface of colloidal Pt) in contrast to the unprotonated one.*

The mechanism of the photoredox reaction of $[BW_{12}O_{40}]^{5-}$ with CH_3OH consistent with our observations involves

$$[BW_{12}O_{40}]^{5-} + CH_3OH \xrightarrow{h\nu} [BW_{12}O_{40}]^{6-} + \dot{C}H_2OH + H^+ \quad (5)$$

$$[BW_{12}O_{40}]^{6-} + CH_3OH \xrightarrow{h\nu} [BW_{12}O_{40}]^{7-} + \dot{C}H_2OH + H^+ \quad (6)$$

$$2[BW_{12}O_{40}]^{6-} \xrightarrow{h\nu} [BW_{12}O_{40}]^{5-} + [BW_{12}O_{40}]^{7-} \quad (7)$$

$$[BW_{12}O_{40}]^{5-} + \dot{C}H_2OH \longrightarrow [BW_{12}O_{40}]^{6-} + HCHO + H^+ \quad (8)$$

$$[BW_{12}O_{40}]^{7-} + 2H^+ \longrightarrow [BW_{12}O_{40}]^{5-} + H_2 \quad (9)$$

$$[BW_{12}O_{40}]^{6-} + H^+ \longrightarrow [HBW_{12}O_{40}]^{5-} \quad (10)$$

$$2[HBW_{12}O_{40}]^{5-} \longrightarrow [BW_{12}O_{40}]^{5-} + [H_2BW_{12}O_{40}]^{5-} \quad (11)$$

$$[H_2BW_{12}O_{40}]^{5-} \longrightarrow\!\!\!\!\!\!\rightarrow [H_xBW_{12}O_{40}]^{(11-x)-} \quad (12)$$

$$[H_2BW_{12}O_{40}]^{5-} \xrightarrow{Pt \text{ or } RuO_2} [BW_{12}O_{40}]^{5-} + H_2 \quad (13)$$

(11)–(13): in strong acidic media

equations (5)—(13). The radical $\dot{C}H_2OH$ produced by ^{60}Co γ-radiolysis reduces $[PW_{12}O_{40}]^{3-}$, $[SiW_{12}O_{40}]^{4-}$, $[FeW_{12}O_{40}]^{5-}$, and $[H_2W_{12}O_{40}]^{6-}$ to the corresponding one-electron reduction species, with a rate constant trend roughly in agreement with the order of the reduction potentials of the oxidized polyoxotungstates.[28] Thus, we propose a redox reaction (8) between $\dot{C}H_2OH$ and $[BW_{12}O_{40}]^{5-}$, probably at a rate close to the diffusion limit due to a exoergonic reaction ($E_{\frac{1}{2}} = -1.1$[29] and -0.51 V *vs.* Ag–AgCl for $\dot{C}H_2OH$ and $[BW_{12}O_{40}]^{5-}$ respectively).

There is a significant asymmetry of bonding to a terminal oxygen compared with the inner oxygen of the BO_4 tetrahedron.[16] Furthermore, the W–O–W bond angles (*ca.* 150°) of the corner-sharing junction between octahedra belonging to different W_3O_{13} groups in the Keggin structure are significantly different from 90°,[30] implying π bonding between tungsten and the bridging oxygen atom, in addition to a terminal oxygen atom in the WO_6 octahedron. Such a WO_6 octahedron results in the deviation from C_{4v} symmetry and allows the appearance of the bridging oxygen-to-tungsten c.t. band as the lowest l.m.c.t. band. Therefore, the weak absorption at 300—350 nm around the edge of the 255-nm l.m.c.t. band may be assigned as a charge transfer from the π-character bridging oxygen to tungsten. The low value of the kinetic isotope effect (Table) suggests that $\dot{C}H_2OH$ is produced *via* $CH_3\dot{O}$, as denoted in equations (14)—(16), on the basis of the mechanism for the photoreduction of alkylammonium isopolyoxomolybdates.[2-4,31-33] The photoreduction of W^{VI} to W^V proceeds *via* u.v.-induced c.t. from the π-character bridging oxygen to W^{VI} at the W^{VI}···O bond with an accompanying transfer of a CH_3OH proton to a second bridging oxygen at the WO_6 octahedral site, followed by interaction of the non-bonding electrons on the methoxide oxygen with the first bridging oxygen leading to a c.t. complex [equation (14)].† The $CH_3\dot{O}$ is derived from an internal electron transfer [equation (15)] in the c.t. complex

* Adsorption of $[H_2BW_{12}O_{40}]^{5-}$ on the catalyst surface seems to result in the stabilization of $[BW_{12}O_{40}]^{7-}$ on the surface due to the process shown below.

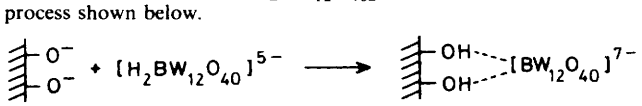

† The photoredox reactions of $[NH_3Pr^i]_6[Mo_8O_{26}(OH)_2]$, $[NH_3Pr]_6[Mo_7O_{24}]$, and $[NH_3Me]_8[Mo_8O_{26}(MoO_4)_2]$ proceed *via* u.v.-induced electron transfer from a terminal oxygen to Mo^{VI}.[31-33] The Mo^{VI} in the photoreducible MoO_6 site of $[Mo_8O_{26}(OH)_2]^{6-}$ and $[Mo_7O_{24}]^{6-}$ is surrounded by a distorted octahedron of six oxygen atoms, two of which are terminal and doubly bonded and four (Mo–O–Mo of *ca.* 100°) of which are bridging.[34,35]

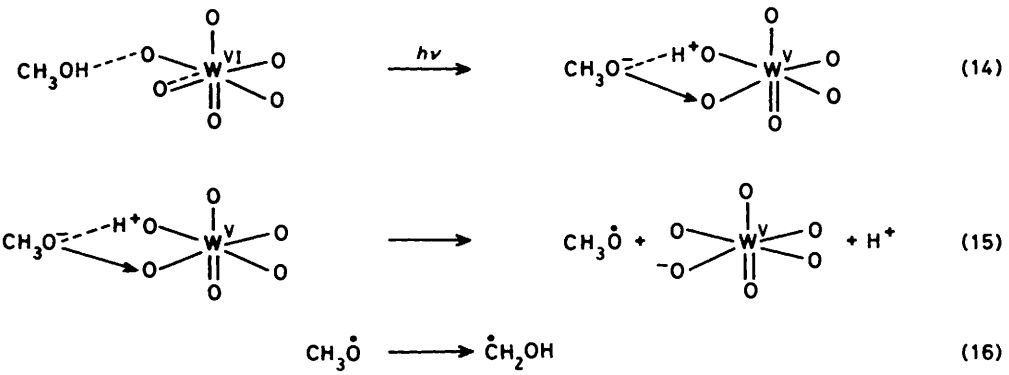

with liberation of $[BW_{12}O_{40}]^{6-}$, in which the d^1 electron will be delocalized to a large extent (Figure 2). Thus, one terminal W=O bond at the WO_6 site would be retained during the photoreaction [equations (14) and (15)], as is supported by the fact that the terminal W=O l.m.c.t. band at 255 nm is hardly effected by the 313-nm photolysis (Figure 1).

As regards the protonation of $[BW_{12}O_{40}]^{6-}$ [equation (10)], the pH dependence of the e.s.r. signal intensity for the photolyte at constant tungsten(V) concentration (Figure 6) enables us to estimate *ca.* 1.5 as the pK_a of $[HBW_{12}O_{40}]^{5-}$, which corresponds to the solution pH giving half of the limiting value (at pH > 2) of the e.s.r signal intensity.

References

1 T. Yamase, N. Takabayashi, and M. Kaji, *J. Chem. Soc., Dalton Trans.*, 1984, 793.
2 T. Yamase and T. Kurozumi, *Inorg. Chim. Acta*, 1984, **83**, L25; T. Yamase, *ibid.*, 1983, **76**, L25; 1982, **64**, L155; 1981, **54**, L165.
3 T. Yamase and T. Kurozumi, *J. Chem. Soc., Dalton Trans.*, 1983, 2205.
4 T. Yamase, R. Sasaki, and T. Ikawa, *J. Chem. Soc., Dalton Trans.*, 1981, 628.
5 T. Yamase, *J. Synth. Org. Chem. Jpn.*, 1985, **43**, 249.
6 R. Akid and J. R. Darwent, *J. Chem. Soc., Dalton Trans.*, 1985, 395; J. R. Darwent, *J. Chem. Soc., Chem. Commun.*, 1982, 798.
7 A. Ioannidis and E. Papaconstantinou, *Inorg. Chem.*, 1985, **24**, 439; E. Papaconstantinou, *J. Chem. Soc., Chem. Commun.*, 1982, 13.
8 E. N. Savinov, S. S. Saidkhanov, V. N. Parmon, and K. I. Zamaraev, *React. Kinet. Catal. Lett.*, 1981, **17**, 407.
9 C. L. Hill and D. A. Bouchard, *J. Am. Chem. Soc.*, 1985, **107**, 5148.
10 T. Yamase and R. Watanabe, 5th Int. Conf. Photochemical Conversion and Storage of Solar Energy, Osaka, 1984, B82(6).
11 C. R. Deltcheff, M. Fournier, R. Franck, and R. Thouvenot, *Inorg. Chem.*, 1983, **22**, 207.
12 M. Filowitz, R. K. C. Ho, W. G. Klemperer, and W. Shum, *Inorg. Chem.*, 1979, **18**, 93; M. A. Fedotov, L. P. Kazanskii, and V. I. Spitsyn, *Dokl. Akad. Nauk SSSR*, 1983, **273**, 1179.
13 E. Borgarello, J. Kiwi, E. Pelizzetti, M. Visca, and M. Grätzel, *Nature (London)*, 1981, **289**, 158.
14 C. A. Parker, *Proc. R. Soc. London, Ser. A*, 1953, **220**, 104.
15 Nippon Yakugakukai (ed.), 'Eiseishikenhoh Chukai,' Kanehara, Tokyo, 1973, p. 1065.
16 J. M. Fruchart, G. Hervé, J. P. Launay, and R. Massart, *J. Inorg. Nucl. Chem.*, 1976, **38**, 1627.
17 R. A. Prados and M. T. Pope, *Inorg. Chem.*, 1976, **15**, 2547.
18 C. Sanchez, J. Livage, J. P. Launay, M. Fournier, and Y. Jeannin, *J. Am. Chem. Soc.*, 1982, **104**, 3194.
19 N. S. Hush, *Prog. Inorg. Chem.*, 1967, **8**, 391.
20 B. Movaghar, L. Schweitzer, and H. Overhof, *Philos. Mag., Part B*, 1978, **37**, 683; R. Bachus, B. Movaghar, L. Schweitzer, and U. Voget-Grote, *ibid.*, 1979, **39**, 27.
21 I. G. Austin and N. F. Mott, *Adv. Phys.*, 1969, **18**, 41.
22 C. Sanchez and J. Livage, *J. Chem. Soc., Dalton Trans.*, 1982, 2439.
23 K. Y. Wong, P. N. Schatz, and S. B. Piepho, *J. Am. Chem. Soc.*, 1979, **101**, 2793; R. Cannon, 'Electron Transfer Reactions,' Butterworths, London, 1980, p. 274.
24 J. A. Dean, ed. 'Lange's Handbook of Chemistry,' 11th edn., McGraw-Hill, New York, 1973, pp. 6—30.
25 D. B. Wiberg and P. C. Ford, *J. Am. Chem. Soc.*, 1969, **91**, 124.
26 A. Bard and L. R. Faukner, 'Electrochemical Method,' Wiley, New York, 1980, p. 218.
27 J. M. Fruchart and G. Hervé, *Ann. Chim. (Paris)*, 1971, **6**, 337.
28 E. Papaconstantinou, *J. Chem. Soc., Faraday Trans. 1*, 1982, 2769.
29 J. Lilie, G. Beck, and A. Henglein, *Ber. Bunsenges. Phys. Chem.*, 1971, **75**, 458.
30 J. Lefebvre, F. Chauvean, P. Doppelt, and C. Brevard, *J. Am. Chem. Soc.*, 1981, **103**, 4589.
31 T. Yamase, *J. Chem. Soc., Dalton Trans.*, 1978, 283.
32 T. Yamase, *J. Chem. Soc., Dalton Trans.*, 1982, 1987.
33 T. Yamase, *J. Chem. Soc., Dalton Trans.*, 1985, 2585.
34 M. Isobe, F. Marumo, T. Yamase, and T. Ikawa, *Acta Crystallogr., Sect. B*, 1978, **34**, 2728.
35 Y. Ohashi, K. Yanagi, Y. Sasada, and T. Yamase, *Bull. Chem. Soc. Jpn.*, 1982, **55**, 1254.

Received 12*th August* 1985; *Paper* 5/1405